

Magnetic Surface Levels in Cu—Determination of Electron-Phonon-Scattering Rates

R. E. Doezema and J. F. Koch

Physics Department, University of Maryland, College Park, Maryland 20742

(Received 2 May 1972)

Using the surface-quantum-state resonances in Cu at microwave frequencies ~ 35 GHz we have investigated the temperature dependence of the electron scattering rate in the range 2–25 °K. From the temperature dependence we obtain the electron-phonon scattering rates of the resonant electrons. We describe the procedure in which we assign a value of the scattering rate to an experimental line shape, and consider how the value of the scattering rate thus obtained is related to a localized group of electrons on the Cu Fermi surface. The ten locations on the Fermi surface at which we have measured the thermal scattering rate are along the central zones of the (100) and (110) planes. We find a maximum-scattering-rate anisotropy of about a factor of 30, the highest rate being on the necks, and the lowest at the $\langle 110 \rangle$ direction.

I. INTRODUCTION

The anisotropy of the electronic scattering rate $\Gamma(\vec{k})$ on the Fermi surface (FS) of metals plays an important role in electronic transport phenomena. It is also very much a problem of current interest in metals research.¹

In this work we elaborate on our preliminary report² of the anisotropic thermal phonon scattering rate for electrons on the FS of copper. The scattering rates are obtained from an analysis of the temperature-dependent line shape of the microwave resonance spectra of magnetic-field-induced surface states,^{3,4} i. e., the surface type of Landau level. In a separate paper⁵ these resonances in Cu have been interpreted and the location of resonant electrons on the FS has been established. We remind the reader that each resonance signal is due to a well-defined group of electrons located on a small striplike zone of the FS. The angular width of this zone is related to the segment of arc traversed by the skipping electron and is typically a fraction of one degree, when measured from the center of the Brillouin zone. The length of the zone of resonant electrons depends on just how sharply the extremal value of the parameter $(K/v_F^2)_\perp$ is defined. K is the radius of curvature and v_F the velocity for the skipping electrons on the FS; both are to be taken in the plane perpendicular to the field H . For more detailed discussion of this point we refer the reader to Ref. 5 and simply assert here that such angular length generally amounts to about 10° in the case of Cu.

The total scattering rate $\Gamma(\vec{k})$ of a surface-state electron is expected to be the sum of all the scattering probabilities $A(\vec{k}, \vec{k}')$ of the state \vec{k} into final states \vec{k}' on the FS, i. e.,

$$\Gamma(\vec{k}) = \int_{\text{FS}} A(\vec{k}, \vec{k}') d\vec{k}' \quad (1)$$

We expect that scattering rates due to various

mechanisms, such as impurities, lattice defects, surface roughness, and thermal phonons are additive. We also expect that all phonon scattering events are catastrophic in the sense that the scattering vector $\vec{k}' - \vec{k}$ in a single event is sufficient to remove the electron from the small strip contributing to the resonance signal. This is evident from the fact that at temperatures on the order of 10°K , characteristic of the temperature range for which we measure the scattering rate, typical phonon wave vectors are on the order of $\frac{1}{30}$ of the Debye wave vector. Consequently the average scattering event displaces the electron by about $\frac{1}{30} k_F$, which is larger than the width of the zone contributing the resonance signal. Furthermore, we must presume that the dominant scattering of the surface states in this temperature range is due to bulk phonons rather than surface modes. Surface phonons at 10°K are expected to be localized to within about 100 \AA of the surface compared to the characteristic penetration of 1000 \AA for the surface electrons. Prange⁶ has examined this question in more detail and reached the same conclusion. Taking account of these arguments, one is led to expect that our measurements should yield a scattering rate of the form

$$\Gamma(\vec{k}) = \Gamma_0(\vec{k}) + \gamma(\vec{k})T^3 \quad (2)$$

$\Gamma_0(\vec{k})$, the temperature-independent part of the total scattering rate, is due to impurities, surface irregularities, and lattice defects. Among the latter, the electron-dislocation line scattering rate has been found to be anisotropic over the Cu FS,⁷ and judging from recent measurements of dilute Au alloys,⁸ impurity scattering likewise should show distinct anisotropy characteristic of the type of impurity.

In the present work we focus attention on the temperature-dependent part of the scattering rate, i. e., we aim to measure the anisotropy of $\gamma(\vec{k})$

over some characteristic zones of the FS of Cu. A first attempt at measuring the anisotropic $\gamma(\vec{k})$ from cyclotron resonance in Cu was made by Häussler and Welles.⁹ They measured the average value of $\gamma(\vec{k})$ over the (100) belly orbit. Their data showed that the scattering closely obeyed a T^3 law as postulated in Eq. (2). They also found, in qualitative agreement with a prediction by Ziman,¹⁰ that $\gamma(\vec{k})$ for the neck orbit is considerably larger than for the belly orbit.

We give first a brief description of the experimental arrangement used to measure and control sample temperature. This is followed in Sec. III by a discussion on how to determine a scattering rate from the experimental resonance spectra. Section IV presents the results of our measurements in Cu. In the concluding comments and discussion of Sec. V we relate these to other measurements and a recent calculation of electron-phonon scattering in Cu.¹¹

II. EXPERIMENTAL ASPECTS

We mention here only those modifications to the usual microwave spectrometer which are necessary for the observation of the temperature dependence of the surface electron resonances.

In our apparatus the temperature of the sample is increased above that of the liquid-helium bath using a noninductive heater wound around the microwave cavity resonator. The cavity itself is mounted at the end of a section of stainless-steel waveguide and inside a can which excludes the liquid helium. Helium exchange gas is admitted to the can at a pressure sufficient to obtain thermal equilibrium in a reasonable time.

Measurement of the temperature is made by using an ac bridge to determine the resistance of a carbon resistor. The resistor is wrapped with copper wire and soldered to a thin strip of copper. Silver print (GC Electronics) is applied to the opposite face of the strip, and the assembly is then clamped to the back of the sample with a phosphor-bronze spring. The resistor is calibrated at three points: 20.4, 4.2, and 2.3°K. Intermediate temperatures are then interpolated from the resistance readings using the formula given by Clement and Quinell.¹² The major source of error in the temperature measurements is the possibility of imperfect thermal coupling of the carbon resistor to the sample. In general, however, the data were quite reproducible with repeated mounting of the resistor to the sample. We expect the uncertainty in temperature readings not to exceed $\pm 1\%$.

III. DETERMINATION OF SCATTERING RATE

We first examine how a value of the scattering rate Γ is assigned to a given resonance spectrum. Subsequently we consider how this scattering rate

is related to a localized group of electrons on the Cu FS.

A. Line-Shape Fitting

In the experiments we study the resonances in the magnetic field derivative of the real part of the surface impedance (dR/dH) as a function of the applied field. Assuming perfectly specular reflection of electrons at the surface, the experimental resonance spectra may be fit to the theory of Nee, Koch, and Prange⁴ with only three parameters: $(K/v_F^3)_\perp$, β , and $\Gamma^* = \Gamma/\omega$. $(K/v_F^3)_\perp$ determines the magnetic field position of the resonances. β is a parameter related to the penetration of the rf fields in the skin layer and it influences the relative amplitude of the individual peaks of the resonance pattern. Γ^* is a lifetime parameter which relates to the width and absolute amplitude of each dR/dH peak. In previously reported work⁵ we have used the dependence of the peak positions on $(K/v_F^3)_\perp$ to measure the distribution of v_F on the FS of Cu and have established the FS location of every extremal value of $(K/v_F^3)_\perp$ for which resonances were observed. In fitting the data to calculation we have also assigned values of β to the spectra.

In the present work we take $(K/v_F^3)_\perp$ and β as known, and vary Γ^* by changing the temperature. We typically encounter values of the parameter Γ^* in the range 0.025–0.125. To illustrate the change of the resonance spectra over this range of Γ^* , we show in Fig. 1 the theoretically predicted dR/dH curves as the parameter Γ^* is varied. β is chosen as 0.5 which is typical of the Cu data. The calculation assumes spherical FS geometry and includes the effects of k_H broadening as discussed in Ref. 5. As in that work, k_H is the wave-number coordinate along the field direction. Also the field scale h is normalized according to this previous work. Note that the spectra in Fig. 1 are dominated by the peak involving the transition from the first to the second energy level, i. e., the 1–2 transition at $h_p \approx 0.435$. In the analysis of data we use this peak in fitting values of Γ^* . The values of Γ^* obtained in this way are least susceptible to error due to distortions from possible overlap of other series. It is also evident that this peak can be observed for the largest range of Γ^* .

Because changes in signal amplitude are difficult to monitor experimentally, we chose the dR/dH peak width of the 1–2 transition as the relevant fitting criterion. Peak width Δh_p is measured at half-amplitude in the manner indicated in Fig. 1. The amplitude A is defined as the separation of the dR/dH peak to the dR/dH minimum on the low-field side. From a set of calculated curves such as those in Fig. 1 we have established that for Γ^* between 0.025 and 0.150 the fractional half-width $\Delta h_p/h_p$, or in real field units $\Delta H_p/H_p$, varies linear-

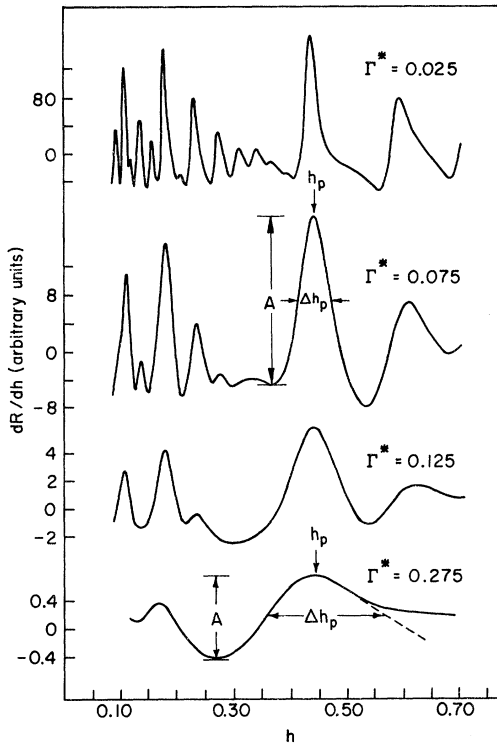


FIG. 1. Computed surface state resonance curves for different values of the lifetime parameter Γ^* . The calculation assumes spherical FS geometry, ideally specular surface reflection, and a value of the skin depth parameter $\beta=0.5$. Resonance amplitude A and position h_p of the $1 \rightarrow 2$ transition, as well as the width at half-amplitude Δh_p , are read off as marked on the figure.

ly with Γ^* for the spherical FS model with $\beta=0.5$. The relation of $\Delta H_p/H_p$ vs Γ^* is shown in Fig. 2. Only above $\Gamma^*=0.2$ is there a substantial deviation from the straight-line relation. We have repeated the calculations using a cylindrical FS model, where the resonance fields of all electrons on the FS are identical, to find also a straight-line relationship (Fig. 2), but valid over a larger range of Γ^* and with zero intercept. The slope of the lines for the two models are substantially the same. We express the relation between linewidth and Γ^* analytically as

$$\begin{aligned} \Delta H_p/H_p &= 1.51\Gamma^* \quad (\text{cylindrical FS}), \\ \Delta H_p/H_p &= 0.02 + 1.56\Gamma^* \quad (\text{spherical FS}). \end{aligned} \quad (3)$$

Because we are primarily interested in changes of linewidth with temperature T , the constant term is of no consequence. The variation of the resonance parameter with k_H in Cu is characteristically that of a sphere for most of the points to be measured. For that reason we will adopt the second of the two relations in (3) above in evaluating the data. The difference of about 3% in the slopes is indica-

tive of the kind of error expected by ignoring the details of the k_H broadening. By repeating the calculations of the cylindrical FS model for $\beta=0.45$ and $\beta=0.55$ we find, respectively, that the slope increases and decreases by about 5%. Ignoring, as we do here, the possible small variation of β for the various different points on the FS that we have studied, is expected to lead to a maximum additional uncertainty of $\pm 5\%$.

B. Interpretation of Measured Γ

Having derived a value of $\Gamma^* = \Gamma/\omega$ by fitting the experimental resonance line, we must ask the question to which electrons on the FS this value of Γ applies. For a cylindrical FS, the answer is that all electrons contained on the entire length of the strip centered about the line $v_x=0$, i.e., electrons whose velocity component normal to surface is zero, contribute equally to the resonance because they all have the same value of the resonance parameter $(K/v_F^3)_1^{1/2}$. The width of the strip, as we have said earlier, is the skipping angle and is on the order of 1° . For a noncylindrical FS, a given resonance line is mostly due to the $v_x=0$ electrons whose value of $(K/v_F^3)_1^{1/2}$ is extremal. However, neighboring electrons with $(K/v_F^3)_1^{1/2}$ values differing slightly from the extremal value also contribute to the line shape. This k_H broadening effect was discussed at length in Ref. 5. It has been shown that electrons whose resonance fields lie within the width of the line contribute effectively to the resonance. The maximum deviation of $(K/v_F^3)_1^{1/2}$ from the extremal value, and hence the effective strip length, can be estimated as

$$\Delta(K/v_F^3)_1^{1/2}/(K/v_F^3)_1^{1/2} \text{ extremal} \approx \Delta H_p/H_p. \quad (4)$$

This relation is subsequently used in Table I to provide an estimate of the length of the strip of

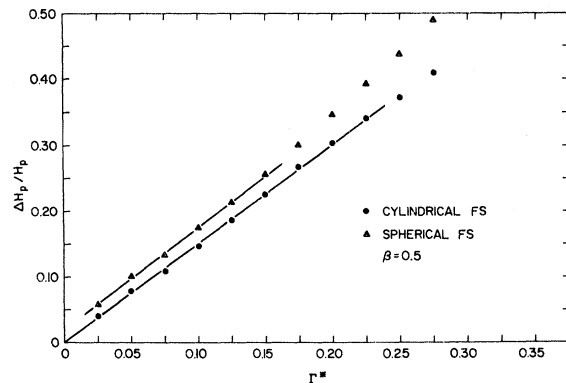


FIG. 2. Variation of the fractional half-width $\Delta H_p/H_p$ for the $1 \rightarrow 2$ transition with lifetime parameter Γ^* for both cylindrical and spherical FS geometry and a value of the skin depth parameter $\beta=0.5$.

TABLE I. Results of fitting the observed scattering rates to $\Gamma = \Gamma_0 + \gamma T^3$. θ is the angle which the magnetic field makes with the $\langle 100 \rangle$ axis, and ϕ is the FS location angle measured from the $\langle 100 \rangle$ axis relative to the zone center. $\Delta\phi$ indicates the length of the zone over which Γ is averaged. The sample to which each value of Γ_0 corresponds is indicated in parentheses.

Zone	θ (deg)	ϕ (deg)	$\Delta\phi$ (deg)	Γ_0 (10^3 sec^{-1})		γ ($10^7 \text{ sec}^{-1}/^\circ\text{K}^3$)
(100)	0	0	± 6	3.0	(A)	1.18 ± 0.08
			± 8	10.8	(B)	1.15 ± 0.04
	15	3.15	+8	11.4	(B)	1.10 ± 0.08
			-7			
	30	6.5	+7	10.3	(B)	1.18 ± 0.10
			-6			
(110)	45	7.5	+6	4.4	(A)	1.19 ± 0.08
			-5			
	0	12.8	± 5	8.5	(B)	0.81 ± 0.05
	15	15.3	+5	7.1	(B)	0.66 ± 0.10
		-3.5				
(110)	0	13.5	+10	5.7	(C)	0.93 ± 0.06
			-5			
	0	69.4	+5	7.9	(D)	1.2 ± 0.2
		-3				
(110)	0	90	± 11	19	(C)	0.12 ± 0.04
(111)	...	Neck	$\sim 0^a$	7.4	(E)	3.60 ± 0.15

^aFor the (111) sample plane where the neck resonance has been studied, the length of the zone subtends an angle of about $\pm 30^\circ$ with reference to the neck center. The width of this zone, however, when viewed from the center of the Brillouin zone, subtends a negligibly small angle. Our measured isotropic value for the scattering rate about the neck is thus taken to apply to the intersection of the neck zone and the (110) zone.

electrons contributing to the resonance.

Another consequence of the relation in Eq. (4) is that as we vary the temperature, the changing linewidth $\Delta H_p/H_p$ implies a changing effective strip length, and hence a change in which electrons contribute to the signal. Given a strong anisotropy of $\gamma(\vec{k})$, this fact could upset the expected temperature dependence of the measured scattering rate. However, judging from the observed characteristic T^3 dependence in the present work in Cu this does not appear to be a very serious problem. Nevertheless, we are forced to the realization that a measured value of γ in this context must be considered as an appropriate average over the vicinity of the point \vec{k} . This is in contrast to our work in Ref. 5 where the calculations allowed us to extract the extremal value of $(K/v_F^3)_L$, hence the value at a point. It is possible in principle to compute the resonance line with some assumed anisotropic $\gamma(\vec{k})$ and to iterate this until detailed agreement with the observed line is obtained, but it would be an exceedingly cumbersome process. An additional complication would be the variation of $\Gamma_0(\vec{k})$. We are content here with the average implied in Eq. (4) and realize that some fine detail in the variation of $\gamma(\vec{k})$ may be obscured

in this way.

IV. EXPERIMENTAL RESULTS

The choice of orientations for which we measure the temperature dependence of the scattering rate is dictated largely by the requirement that the $1 \rightarrow 2$ transition peak be not seriously perturbed and distorted by peaks from other resonance series. This "clean-signal" restriction does not seriously hamper our work in the (110) and (111) sample planes, but it limits us to only three FS locations in the (110) plane. For a more complete picture of signal anisotropies we refer the reader to Ref. 5.

A sequence of dR/dH traces for three different temperatures appears in Fig. 3. The data are due to electrons at the $\langle 100 \rangle$ point of the FS, i.e., that point intersected by the $\langle 100 \rangle$ axis. The changes with increasing T and Γ^* closely parallel the theoretical curves in Fig. 1. From such experimental curves we extract a value of $\Delta H_p/H_p$, which in conjunction with Eq. 3 gives $\Gamma^*(T)$. As mentioned earlier we make use of the relation between linewidth and Γ^* appropriate for spherical FS geometry. The locally spherical shape of the FS near the $\langle 100 \rangle$ point makes this a good representation.

We also find a convincing fit of such data on the $\langle 100 \rangle$ point signal to the T^3 relation postulated

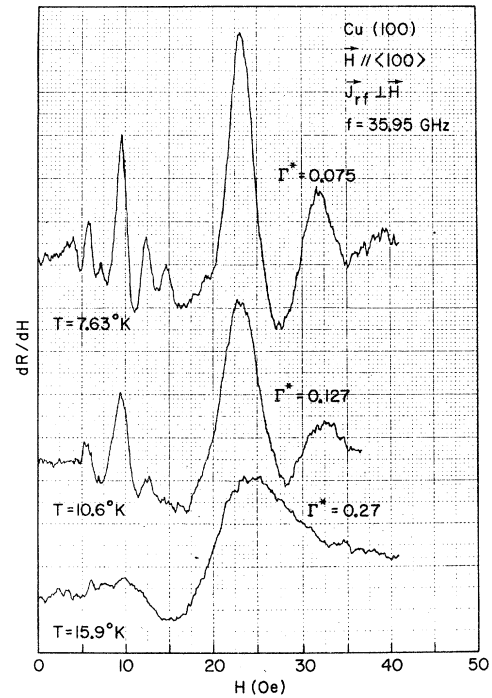


FIG. 3. Experimental curves for the $\langle 100 \rangle$ point resonance at different temperatures. These spectra are to be compared with the theoretical curves in Fig. 1. Γ^* values are derived from the measured fractional half-width.

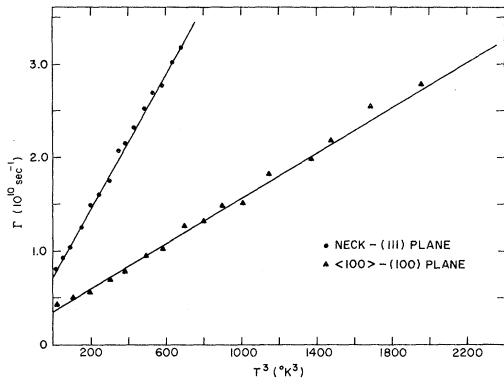


FIG. 4. Plot of experimental values of $\Gamma = \Gamma^*\omega$ vs T^3 for the neck and $\langle 100 \rangle$ point on the FS of Cu.

earlier in Eq. (2). Plotted as a function of T^3 we find the straight line shown in Fig. 4, with the scatter not exceeding reasonable experimental uncertainty. An equally good fit to Eq. (2) is evident for the data on the neck point also shown in Fig. 4. The T^3 relation is found to represent data from the other FS locations as well. We have fit our data to an equation of the form $\Gamma = \Gamma_0 + \gamma T^x$ with Γ_0 , γ , and x chosen to provide a least mean square fit to the data points. We find the average value for x as 3.0 ± 0.2 . We subsequently fit all data assuming an accurate T^3 variation and determine the anisotropy of the coefficient γ on the FS of Cu.

As a check on our experimental procedure and method of analysis we have carried out the $\langle 100 \rangle$ point measurements in a number of samples with substantially different residual scattering and different surface preparation. The residual scattering as measured by Γ_0 varied by as much as a factor of 3 between these samples but the coefficient γ was entirely reproducible. This is also proof of the applicability of Matthiessen's rule in this limit of very dilute impurity concentrations.

Another more sophisticated check involved frequency scaling of the $\langle 100 \rangle$ point data. The sample is mounted on the cylindrical cavity resonating at 28.0 and 37.5 GHz in the TE_{111} and TE_{112} modes, respectively. Thus, in the same run we are able to measure the parameter Γ^* and check for the expected $1/\omega$ scaling. Surface condition, orientation, direction of rf currents (J_{rf}) and temperature are of course identical. We have found that the slopes in the plot of Γ^* vs T^3 , i. e., γ/ω , scaled exactly as expected. The temperature-independent part, i. e., the γ intercept Γ_0/ω , failed to obey the scaling precisely. The latter is expected to be the case because of the approximation to the actual FS geometry implied by the spherical FS model calculations in Fig. 1 and Eq. (3) which were used to interpret the data. Lack of exact frequency scaling of Γ_0/ω could also result from a small field-depen-

dent part of the scattering due to surface roughness or surface undulations such as those discussed in Ref. 5.

In Fig. 5 and Table I, we summarize our results for γ values at representative points in the (100) and (110) zones. The γ values for seven of these points were in our preliminary report on this work.² Except for the $\phi = 13.5^\circ$ location in the (110) zone, the present results are essentially unaltered except for corrections in the location angle which are the result of our more detailed study of surface states in Cu.⁵ There are also slight corrections in the values of γ because of a better determination of the slope in Eq. (3). We were unable to reproduce our earlier value of γ at the $\phi = 13.5^\circ$ location in the (110) plane. A number of temperature runs in the same and in a second (110) sample yielded the present value in Table I. It is likely that the earlier incorrect result was due to poor thermal contact between the sample and the carbon resistance thermometer. As in Ref. 5, the angle θ in Table I gives the orientation of the magnetic field for which the resonance is observed. The angle ϕ denotes the location of the electrons on the FS. Both are measured from the $\langle 100 \rangle$ axis and with respect to the center of the Brillouin zone. The column $\Delta\phi$ represents the angular length of the strip over which the γ value is an average. Values of $\Delta\phi$ are based on the estimate in Eq. (4) using the actual variation of the resonance parameter $(K/v_F^3)_L^{1/2}$ along the zone and about the extremal value. Each value listed in the table represents

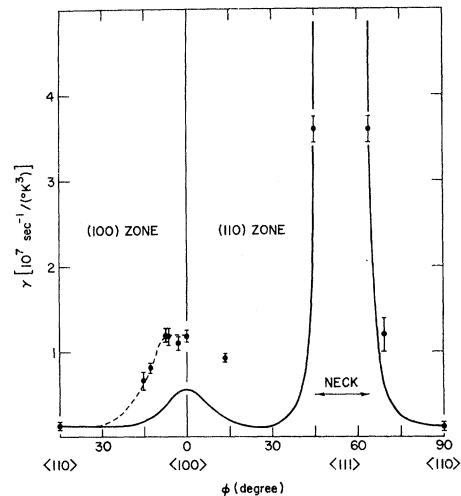


FIG. 5. Variation of the thermal phonon scattering parameter $\gamma(\vec{k})$ on the (100) and (110) central zones of the FS of Cu. ϕ is the angle between \vec{k} and the $\langle 100 \rangle$ axis. The dashed line is drawn smoothly through the experimental points and is used to calculate an orbital average of the relaxation rate. The solid line gives the result of a recent calculation by Nowak and Lee.

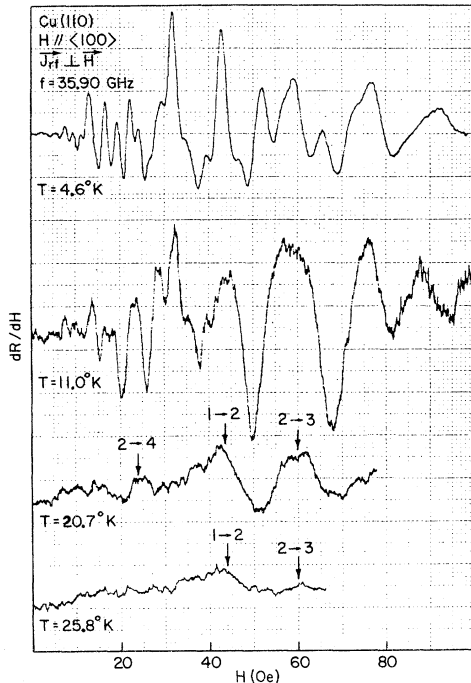


FIG. 6. Experimental curves for H along the $\langle 100 \rangle$ axis in the (110) plane of Cu using the perpendicular mode of current polarization. Signals from the $\langle 110 \rangle$ point can only be identified for $T > 15^\circ\text{K}$. Individual peaks of this signal are marked with arrows in the two lower traces.

an average over the range of $\Delta\phi$ computed from the variation in $\Delta H_p/H_p$ corresponding to each run for temperatures below 10°K . Values of Γ_0 are tabulated to indicate the order of magnitude of the temperature-independent scattering rates for the various directions. The corresponding samples are indicated in parentheses after each value of Γ_0 . Samples A and D were cut from the same boule as were C and E . Because our analysis ignores the detailed k_H broadening for each of the points we cannot be sure that these Γ_0 values represent an anisotropy of residual impurity and defect scattering. Moreover the nature and concentration of impurities and defects are not known.

The two locations in the (110) plane where we have obtained values of γ merit some discussion. All three locations in this plane are measured with the magnetic field along the $\langle 100 \rangle$ axis. For the microwave current polarized parallel to the field only the spectrum from the $\phi = 13.5^\circ$ location is observed⁵ and its γ is then measured in the usual way. For the perpendicular mode of polarization all three FS locations give rise to observable signals. The $\langle 110 \rangle$ point ($\phi = 90^\circ$) signal is so weak that it is observable only at temperatures above 15°K , for which the other two signals have been attenuated because of their relatively stronger phonon scat-

tering. The experimental traces for this orientation and the perpendicular polarization mode appear in Fig. 6. The traces clearly exemplify the difficulties involved in separating out the different signals and explain the relatively large error bars for the γ value in this orientation. As apparent from the figure, the $\langle 110 \rangle$ point signal persists to temperatures in excess of 25°K because of its exceedingly low phonon scattering rate. Its γ value is determined from such high temperature curves. The γ value for $\phi = 69.4^\circ$ is obtained by subtracting from the perpendicular polarization traces (Fig. 6) an appropriate fraction of the parallel-mode trace which contains only one of the signals. The linewidth of the $1 \rightarrow 2$ peak is measured after this subtraction.

The neck relaxation rate is studied most easily in the (111) plane sample, where the neck signal predominates. With field rotation in this sample plane the extremal point moves around the neck. No anisotropy of the neck scattering rate is evident in such a sequence of runs. It would appear that the γ value for electrons on the neck is indeed isotropic, but because our measurement averages over a finite length of strip on the neck, the possibility of some small amount of variation of γ cannot be excluded.

The error bars for γ indicated in Fig. 5 and in Table I represent an estimate of possible error based on uncertainty in the temperature measurements, uncertainties in the linewidth because of noise or overlapping peaks, and finally the approximation implied by the use of Eq. (3), which treats the k_H anisotropy for spherical FS geometry. An additional source of error, not included in the estimate, is the effect of the possible variation in the value of β .

V. DISCUSSION AND CONCLUSIONS

The anisotropy of the strength of the electron coupling to thermal phonons, as evidenced by the data in Fig. 5, is a remarkable result. The variation of the coefficient of the T^3 term in the scattering rate is found to extend over a factor of 30. We have just recently been made aware of an effort at a theoretical explanation and calculation of this anisotropy. The result of Nowak and Lee,¹¹ which we have included in Fig. 5 appears to give a satisfactory account of our measurements. We refer the reader to their work for a discussion of the various factors that enter in the consideration of this scattering rate anisotropy.

We can numerically compare our scattering rates with those that Häussler and Welles⁹ (HW) obtained in an Azbel'-Kaner cyclotron resonance experiment. The value of γ measured in cyclotron resonance represents an orbital average of the form

$$\langle \gamma \rangle = \oint_{\text{orbit}} \left(\frac{\gamma(\vec{k})}{v_{F\perp}} \right) dk / \oint_{\text{orbit}} \left(\frac{1}{v_{F\perp}} \right) dk, \quad (5)$$

where dk is the path-length element. In cyclotron resonance there is additional averaging over various cyclotron orbits with masses near the extremal value. This latter average is similar to the k_H broadening which causes the surface state value of γ to be an average over a strip of finite length on the FS.

Because v_F is constant around the neck, and since we observe a constant value of γ around the neck, our result and that of HW can be compared directly. We find $\gamma = (3.60 \pm 0.15) \times 10^7 \text{ sec}^{-1}/^\circ\text{K}^3$, while HW give $\gamma = 2.7 \times 10^7 \text{ sec}^{-1}/^\circ\text{K}^3$ with an estimated accuracy of a factor of 2. Considering error limits there is agreement. For a comparison with the (100) belly orbit we must average our γ values using Eq. (5). To do so, we draw a smooth curve through our experimental values of γ in the (100) zone (dotted line in Fig. 5) and using the known velocity distribution in Cu we obtain $\langle \gamma \rangle = 0.50 \times 10^7 \text{ sec}^{-1}/^\circ\text{K}^3$, while HW give $\langle \gamma \rangle = (0.29 \pm 0.12) \times 10^7 \text{ sec}^{-1}/^\circ\text{K}^3$. These two results seem to disagree by more than the quoted error limits. The difference should not be considered irreconcilable, however, because we have found it necessary to extrapolate γ over much of the orbit. Also because the cyclotron mass is quite stationary as a function of k_H for this orienta-

tion, the HW value is an average over a wide band of orbits about $k_H = 0$. Our data shows that scattering decreases away from the $\langle 100 \rangle$ point and hence a lower value of $\langle \gamma \rangle$ for cyclotron resonance is expected.

In concluding we would like to emphasize that the present exploration of scattering rate anisotropy was made possible by our knowledge of the locations of resonant electrons on the FS of Cu. These locations were obtained in our previous work⁵ and made use of the accurately known FS geometry. The latter is thus a prerequisite for undertaking similar studies of relaxation time anisotropy in other metals. In addition, it must be remembered that our analytical procedure has led to a scattering rate value which is a weighted average over a small but finite length of strip on the FS. The extent of this averaging, however, is not sufficient to mask the strong anisotropy over the (100) and (110) zones.

As a final note, we remind the reader that our analysis of the data has relied heavily on the line-shape theory and calculations of Nee, Koch, and Prange.⁴ While these calculations on the whole correspond closely to the experimental curves, some minor discrepancies remain and are probably the result of the various approximations made in the calculation. To the extent that these affect the line shape they would have an influence on the present results.

¹For an up to date review of scattering anisotropy in the noble metals see M. Springford, *Advan. Phys.* **20**, 493 (1971).

²J. F. Koch and R. E. Doezema, *Phys. Rev. Letters* **24**, 507 (1970).

³R. E. Prange and T. W. Nee, *Phys. Rev.* **168**, 779 (1968).

⁴T. W. Nee, J. F. Koch, and R. E. Prange, *Phys. Rev.* **174**, 758 (1968).

⁵R. E. Doezema and J. F. Koch, *Phys. Rev. B* **5**, 3866 (1972).

⁶R. E. Prange, *Phys. Rev.* **187**, 804 (1969).

⁷D. W. Terwilliger and R. J. Higgins, *Phys. Letters* **31A**, 316 (1970).

⁸D. H. Lowndes, K. Miller, and M. Springford, *Phys. Rev. Letters* **25**, 1111 (1970).

⁹P. Häussler and S. J. Welles, *Phys. Rev.* **152**, 675 (1966).

¹⁰J. Ziman, *Phys. Rev.* **121**, 1320 (1961).

¹¹D. Nowak and M. J. G. Lee, *Phys. Rev. Letters* **28**, 1201 (1972); and D. Nowak, *Phys. Rev. B* (to be published).

¹²J. R. Clement and E. H. Quinell, *Rev. Sci. Instr.* **23**, 213 (1952).